Nature and Location of Organic Species in As-Synthesized Ferrierite Probed by Near-Infrared Fourier Transform Raman Spectroscopy and Multinuclear NMR

A. Davidson,*,† S. J. Weigel, L. M. Bull, and A. K. Cheetham

Materials Research Laboratory, University of California, Santa Barbara, California 93106

Received: September 26, 1996; In Final Form: February 4, 1997[⊗]

Siliceous and aluminosilicate ferrierite samples (Si/Al ratios = 18, 50, and 80) have been prepared in the presence of propylamine and pyridine and characterized by near-infrared Fourier transform Raman spectroscopy and ^{29}Si, ^{27}Al, and ^{13}C NMR. Incorporation of aluminum into the framework has two main consequences. Firstly, propylammonium cations partially charge compensate for the aluminum substitution in the framework. As a consequence of this, as the Si/Al ratio is lowered and the number of propylammonium cations required for charge neutrality increases, the concentration of pyridine in the main channel decreases because the two molecules compete for space in the zeolite channels. Secondly, two types of pyridine are observed from the splitting of the ν_1 breathing mode. This is proposed to arise from pyridine physically adsorbed in the 8-ring side channel and the main 10-ring channel (ν_1= 991 cm^{-1}) and pyridine located in the main channels interacting via hydrogen bonding with propylammonium cations (ν_1 near 1000 cm^{-1}). In agreement with this postulate, the proportion of hydrogen-bonded pyridine molecules increases as the aluminum concentration and the number of charge-compensating propylammonium cations increases.

Introduction

Crystalline silica-based zeolites with unique architectures can be synthesized under hydrothermal conditions using carefully selected nitrogen-containing bases as organic templates.[1] The role of these bases has been widely discussed in the literature, although no general principles have yet emerged.[2] It has been proposed for some reactions that the base acts as a structure-directing agent[3] or is involved in forming preorganized inorganic−organic composites in the early stages of reaction,[4] while in other reactions the base may purely modify the gel chemistry.[5] In this context, characterization of the organics trapped inside as-synthesized zeolites will be necessary for understanding the interactions between the guest and the host and may ultimately lead to a better understanding of the role of organic bases in zeolite synthesis. With this aim in mind, infrared spectroscopy should be a powerful characterization tool and indeed has been used extensively to study organic molecules adsorbed on inorganic substrates.[6] However, the use of IR spectroscopy to study zeolite systems has been limited by absorptions from framework vibrations obscuring large regions of the infrared spectra, including the ranges typically associated with vibrations of organic molecules. Raman spectroscopy is more informative because framework vibrations, characterized by low-scattering cross sections, are virtually eliminated from the spectra, whereas organic molecules, being strong scatterers, give intense and narrow Raman absorptions.[7] Despite these advantages, to date, Raman spectroscopy has only played a minor role in studies of zeolite crystallization,[8−10] probably because of experimental difficulties associated with conventional Raman spectrometers and severe fluorescence problems.[11] Recent advances in near-infrared Fourier transform (near-IR-FT) Raman spectroscopy[12] have allowed alignment procedures to be simplified and facilitated rapid data acquisition, thereby minimizing the problems of sample instability during measurements. In addition, the wavelength of the incident laser beam, fixed at 1100 nm, which is known to induce strong heating effects for colored samples,[13] is not a drawback with zeolites as these materials are typically colorless. Furthermore, recent studies have demonstrated that little laser-induced fluorescence is produced when a near-IR excitation laser is used.[13]

The present study focuses on ferrierite,[14a] a member of the pentasil family of zeolites which includes mordenite and ZSM-5. The ferrierite structure can be prepared in the absence of inorganic cations.[14b−16] Its architecture is based on five-ring building units, stacked in the [001] direction. These are connected to form oval 10-ring channels running parallel to [001], which are intersected by 8-rings, centered at 0,0,0 (Figure 1). A recent single crystal X-ray diffraction and NMR study[15] of template-containing siliceous ferrierite has shown that both pyridine and propylamine are trapped inside the framework, a result that is corroborated by another study of the same system by Lewis *et al.*[16] Pyridine is located inside the main channel and in the side channel of the structure; the relative populations of these two sites were found to be 0.9:1.0, respectively. Propylamine was found in the main channel at the same site as the pyridine. The relative occupancies at this site for the two organics were refined to be 0.9 and 0.1 for pyridine and propylamine, respectively. ^{13}C NMR clearly shows the presence of pyridine and propylamine in an overall ratio of 20:1, in good agreement with the model obtained from the diffraction data. A trace amount of propylammonium is also present in the ^{13}C NMR spectrum, but it is unclear whether this cation is trapped within the framework after participating in the structure formation or whether it is propylammonium hexafluorosilicate, which is produced in significant amounts during the reaction and was not removed even after thorough washing of the sample with water. As yet, no crystal structure on an aluminosilicate ferrierite synthesized from a fluoride media has been published, and more importantly, no information regarding the incorporation of organics, and the nature of the charge compensation in the structure, is available. Previous work, however, has used Raman spectroscopy to address the role of organics in the aqueous synthesis of aluminosilicate ferrierite.[9] In this study we demonstrate the power of near-IR-FT Raman spectroscopy for the characterization of organics trapped within the ferrierite framework first by showing that the results from as-synthesized

† Permanent address: Laboratoire de Réactivité de Surface (URA 1106-CNRS), Université Pierre et Marie Curie, Paris 75230 Cedex, France.

[⊗] Abstract published in *Advance ACS Abstracts,* March 15, 1997.

S1089-5647(96)02967-7 CCC: $14.00

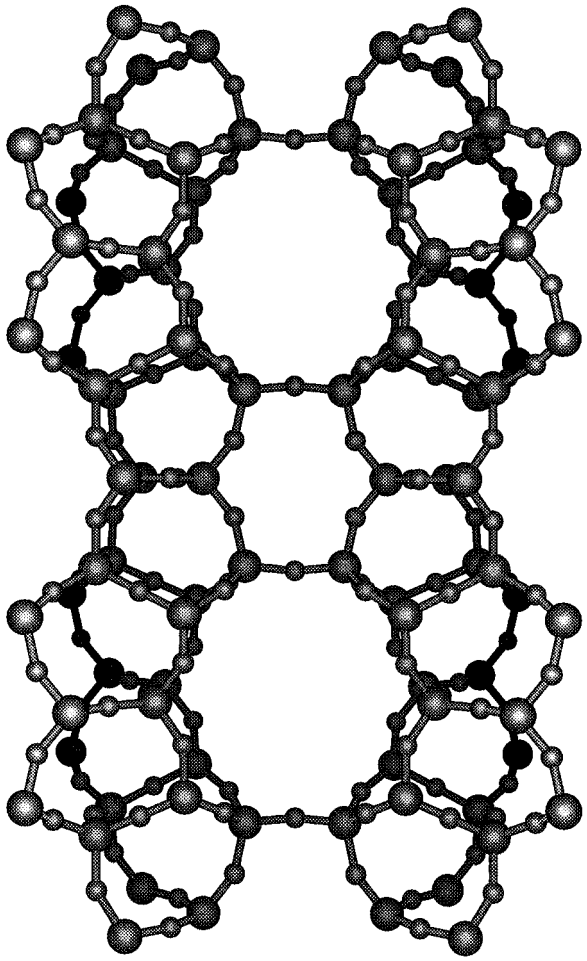

Figure 1. Structure of ferrierite viewed down the [001] direction showing the 10-ring main channels.

siliceous ferrierite are in excellent agreement with the NMR and diffraction study and second by studying the effect on the trapped organics of incorporating aluminum into the framework. The nature of the charge-balancing cations is also addressed.

Experimental Section

Synthesis. The siliceous ferrierite (Si-FER) was prepared by the fluoride route described by Kuperman *et al.*[17] using Cab-O-Sil (Acros—M5 grade), propylamine (Aldrich), pyridine (Fisher), HF-pyridine (Aldrich—70 wt % HF), and deionized water. Three aluminosilicate ferrierites were obtained using the same precursors and similar reaction conditions. Sodium aluminate (Spectrum—28.4 wt % Na_2O, 46.7 wt % Al_2O_3) was used as the aluminum source. Three gels compositions were prepared with molar ratios of

Si/Al = 50:
1.5 SiO_2:2 HF/pyr:0.015 Al_2O_3:0.015 Na_2O:4 $PrNH_2$:8 H_2O:16 pyr

Si/Al = 25:
1.5 SiO_2:2 HF/pyr:0.03 Al_2O_3:0.03 Na_2O:4 $PrNH_2$:8 H_2O:16 pyr

Si/Al = 12.5:
1.5 SiO_2:1.8HF/pyr:0.06 Al_2O_3:0.06 Na_2O:4.1 $PrNH_2$:8.4 H_2O:16.2 pyr

The appropriate amounts of propylamine, pyridine, HF-pyridine, and Cab-O-Sil were combined and stirred until the silica was completely dissolved. An intermediate solution, obtained by dissolving sodium aluminate in deionized water in a separate container, was then added, and the final mixture was stirred for 2−3 h under ambient conditions. The resulting gels were then sealed in 45 mL Parr digestion bombs. The bombs were placed into a 170 °C forced draft oven for 7−10 days. After the bombs were quenched in cold water, their contents were filtered, washed with 500 mL of hot deionized water, and rinsed with acetone.

Characterization. The identification and purity of all samples were established from powder X-ray diffraction, using a Scintag PADX diffractometer and CuKα radiation (40 mA and 45 kV). More than 30 reflections were observed within the range $9° < 2\theta < 60°$ and used for primary indexing and determination of the ferrierite lattice parameters (Table 1). The results from elemental analyses (Galbraith Laboratories, Knoxville, TN) of the aluminosilicate ferrierite samples are also shown in Table 1. The samples had initial gel compositions of Si/Al 50, 25, and 12.5; the corresponding final Si/Al ratios were 80, 50, and 18. For the remainder of this paper, samples will be referred to by the Si/Al ratio of the final product. All the samples contain sodium (Na/Al $\sim$ 0.4), but it was not sufficient for complete charge compensation of the incorporated aluminum.

NMR spectra were recorded on a Chemagnetics CMX-500 spectrometer, operating at frequencies of 129.9 MHz for aluminum and 99.6 MHz for silicon using a double-resonance magic angle spinning probe (7.5 mm o.d. rotors). The ^{27}Al spectra were referenced to a 1 M solution of $Al(NO_3)_3$ at 0 ppm, and the ^{29}Si spectra were referenced to tetramethylsilane, also at 0 ppm. Typical recycle delays of 1 and 300 s for ^{27}Al and ^{29}Si, respectively, were found to be necessary in order that the signals were not saturated. Samples were typically spun at 6.5 kHz. ^{13}C NMR spectra were collected on a Chemagnetics CMX-180 spectrometer at a frequency of 45.30 MHz with decoupling of protons during acquisition. These spectra were referenced also to tetramethylsilane at 0 ppm. A recycle time of 15 s was found to give intensities that were considered to be quantitative.

The near-IR-FT Raman spectra were measured with 4 cm^{-1} resolution on a Nicolet Magna 850 spectrometer equipped with a near-infrared Raman accessory, using a 1064 nm excitation source (Nd:YVO_4). The Raman spectra were recorded at room temperature, by the coaddition of 1000−2000 scans with a laser power ranging between 300 and 900 mW on the sample.

The majority of Raman data in the literature taken from as-synthesized zeolites are measured using dispersive Raman spectrometers with an excitation laser in the visible region (typically 500 nm).[8−10] FT-Raman, working with an excitation laser near 1000 nm, should be less sensitive, but despite this lower sensitivity, the FT-Raman accessory gives a better signal-to-noise ratio. There appear to be two main reasons: (i) the interferometer does not contain any slits or dispersive elements, and so a larger signal reaches the detector, and (ii) dispersive instruments use a single detector, typically a photomultiplier tube where each spectral element is measured sequentially, whereas an FT accessory measures all the spectral elements simultaneously resulting in significantly higher signal-to-noise ratios for identical measurement times.[11]

Results and Discussion

The effect of incorporating Al into the ferrierite framework is demonstrated in Figure 2, in which the ^{29}Si MAS NMR

TABLE 1: Summary of Chemical Analysis and X-ray Powder Diffraction Data

	nominal composition		actual composition		unit-cell parameters (Å)			
sample	Si/Al	Na/Al	Si/Al	Na/Al	*a*	*b*	*c*	volume (Å^3)
18	12.5	1	17.8	0.4	18.90	14.09	7.44	1981
50	25	1	51.4	0.3	18.85	14.09	7.42	1971
80	50	1	79.8	≈0	18.84	14.08	7.43	1970
Si-FER	−	−	−	−	18.82	14.10	7.43	1971

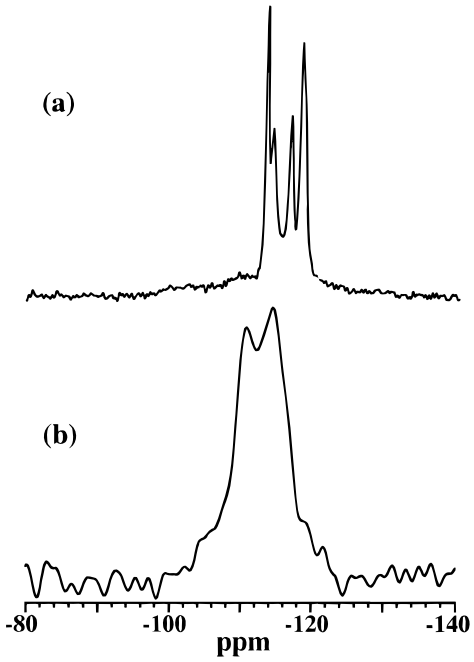

Figure 2. ^{29}Si MAS NMR spectra of templated (a) siliceous ferrierite and (b) aluminosilicate ferrierite (Si/Al = 18) (*y* axis: in arbitrary units).

spectra from Si-FER is compared with the spectrum from the aluminosilicate ferrierite with Si/Al = 18. The spectrum of the siliceous ferrierite consists of at least five narrow but overlapping resonances, indicating at least five structurally nonequivalent Si atoms in the asymmetric unit, consistent with the model from the diffraction data.[15] The spectrum taken from the aluminosilicate ferrierite is considerably broader because of the disorder around each silicon site created by substitution of aluminum into the framework. Simulations of this line shape based on the method described in ref 18 indicate that the Si/Al ratio is within the range of 15−20, in agreement with the elemental analysis. Figure 3 shows the ^{27}Al MAS NMR spectra of the aluminosilicate samples. One resonance at ∼45 ppm, characteristic of tetrahedrally coordinated Al, is observed for all three samples, consistent with aluminum in the samples being incorporated into the framework.

The near-IR-FT Raman spectra of propylamine (pK_a = 10.7), pyridine (pK_a = 5.5), propylammonium fluoride (HF-propylamine solution, pH = 3), and pyridinium fluoride (HF-pyridine solution, pH = 3) are presented in Figure 4, and the main absorptions are listed in Table 2 and assigned according to ref 19a. These spectra are similar to ones measured using a conventional Raman spectrometer using an excitation laser in the visible region.[9,10] For the purposes of this paper, a detailed analysis of the spectra will not be presented; only spectral features important for the identification of the organics present during the ferrierite crystallization will be considered.

Figure 4a shows the near-IR-FT Raman spectrum of propylamine. The aliphatic tail gives prominent absorptions at 2964, 2938, 2876, and 2733 cm^{-1} (CH stretching vibrations) and near 1450 cm^{-1} (overlapping of the −CH_3 antisymmetric deformation and of the −CH_2− scissors vibrations). The most characteristic

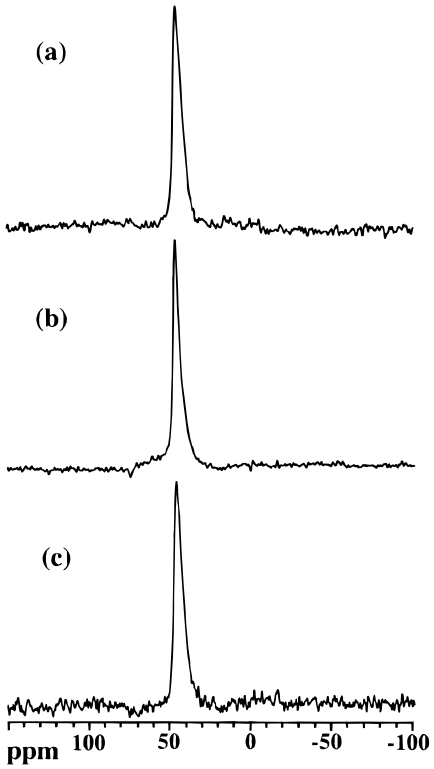

Figure 3. ^{27}Al MAS NMR spectra of the samples with final composition Si/Al molar ratios of (a) 18, (b) 50, and (c) 80 (*y* axis: arbitrary units).

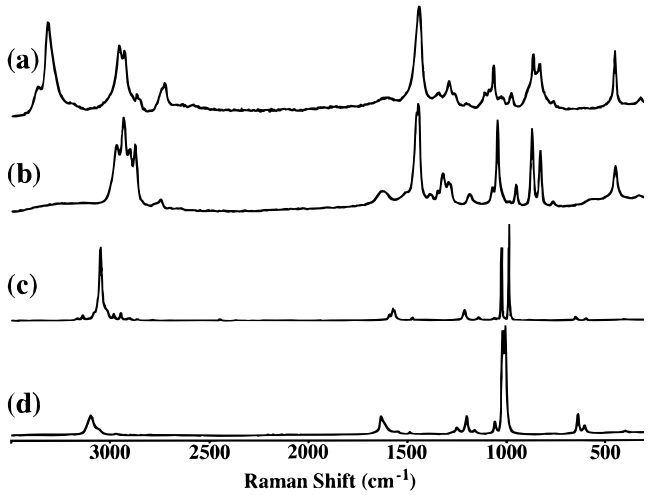

Figure 4. Near-IR-FT Raman spectra of (a) propylamine (liquid), (b) HF-propylamine aqueous solution (pH = 3), (c) pyridine (liquid), and (d) HF-pyridine aqueous solution (pH = 3) (*y* axis: arbitrary units).

peak of liquid propylamine is a broad absorption near 3370 cm^{-1}, associated with an −NH stretching vibration, perturbed by hydrogen bonding. In very dilute solutions, where intermolecular hydrogen bonds are eliminated, this −NH stretching vibration is shifted to higher frequency, typically within the range 3400−3450 cm^{-1}. The spectrum of propylammonium, shown in Figure 4b, is significantly different in the −NH

TABLE 2: Attribution of the Principal Raman Absorptions Observed in Figures 4, 5, and 6

approximate description of vibration (ref 19)	liquid or diluted solutions	sample (Si/Al) 18	50	80	Si-FER
Propylamine					
NH stretch	3370	–	–	–	3330
CH stretch	2964, 2733	–	–	–	–
	2938, 2876	–	–	–	2946, 2880
CH_3 deformation and CH_2 scissors	1450	–	–	–	1450
Propylammonium					
NH^+ stretch	3300	3300	3300	3300	3300
NH_3^+ sym stretch	2976	2974	2974	2974	2974
CH stretch	2941, 2884	–	2939	2935	2935
	2750	–	2882, 2750	2880, 2750	2880, 2750
Pyridine					
CH stretch (ν_2)	3054	3068	3068	3067	3062
ring stretch (ν_{8a},ν_{8b})	1581, 1574	1595, 1575	1583, 1574	1596, 1575	1596, 1574
ring breathing					
trigonal (ν_{12})	1031	1032	1031	1032	1033
symmetric (ν_1)	991	991, 1001	991, 1001	991, 1001	991, 998
Pyridinium					
CH stretch	3099				
ring breathing					
trigonal	1023	not observed			
symmetric	1010				
NH^+ deformation	1250				

stretching region. Protonation of the amine broadens the peak near 3300 cm^{-1} so that it can no longer be readily detected. An absorption at 2976 cm^{-1}, overlapping with the C−H stretching vibrations, is attributed to the symmetric stretch of the NH_4^+ group.

The spectrum of pyridine is more complex (Figure 4c), and so numbering of the vibrations of this molecule will be helpful in the forthcoming discussions. Using the notation proposed by Wilson for benzene,[19] the peak located at 3054 cm^{-1} is assigned to the aromatic C−H stretches (ν_2). The doublet (ν_{8a}, ν_{8b}) at 1581 and 1574 cm^{-1} is due to ring stretches and involves mainly C−C bonds. The two most intense Raman peaks at 991 and 1031 cm^{-1} are assigned, respectively, to the symmetric (ν_1) and the trigonal (ν_{12}) ring-breathing modes. The splitting between these last two peaks, labeled Δ hereafter, is a sensitive probe of protonation of the pyridine or when pyridine participates in hydrogen bonding. For example, a Δ of ∼40 cm^{-1} is common in systems where pyridine−pyridine interactions occur, i.e. liquid pyridine,[20] pyridine physically adsorbed on a surface,[13] and pyridine molecules isolated in an argon matrix.[21] By contrast, Δ for a pyridine/water mixture where a hydrogen-bonded H_2O−pyridine complex is formed is smaller at ∼35−30 cm^{-1}.[21] Similarly, for pyridine adsorbed on oxides where H-bonding is present, a Δ value of 32 cm^{-1} has been observed.[13,22] The formation of pyridinium cations, induced by acidifying an aqueous solution of pyridine with HF until the pH of the solution is 3, also has an effect on Δ, decreasing the splitting still further to 13 cm^{-1} (Figure 4d). Low values of Δ (15−10 cm^{-1}) have also been reported for pyridine interacting with surface Brönsted acid sites of alumina.[23] In addition to this characteristic decrease of the Δ splitting upon formation of pyridinium cations, an additional absorption at 1250 cm^{-1} due to a N−H in plane deformation occurs, and a shift of the C−H stretching vibration from 3054 cm^{-1} in liquid pyridine to 3099 cm^{-1} is observed.

Although pyridine is mainly sensitive to interactions with proton donors, the position of the ν_1 ring-breathing mode of pyridine is also helpful for the diagnosis of other kinds of interactions. For example, the ν_1 mode will be located in the range 1016−1025 cm^{-1} if pyridine coordinates to electron deficient aluminum centers acting as Lewis acid sites.[13,23]

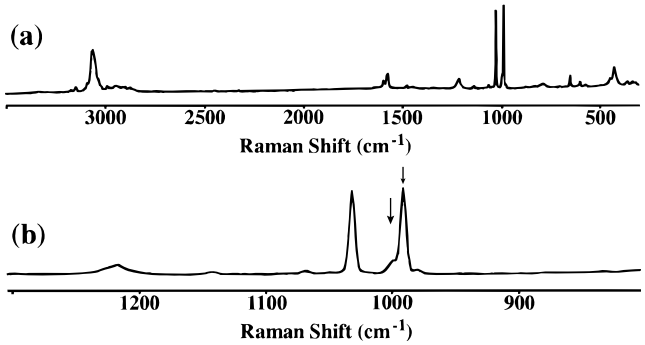

Figure 5. (a) Near-IR-FT Raman spectrum of siliceous ferrierite; (b) an expanded region of the spectrum showing the splitting of the pyridine ν_1 band (y axis: arbitrary units).

The near-IR-FT Raman spectrum of the as-synthesized siliceous ferrierite is shown in Figure 5a. The spectrum is strikingly well resolved, showing comparable resolution to the spectra collected from the liquid organic standards. By comparing Figures 4 and 5, it can readily be seen that the predominant absorption at ∼3062 cm^{-1} and the strong peaks within the range 1050−950 cm^{-1} arise, respectively, from the −CH− stretching and the ring-breathing modes of neutral pyridine. No peaks from pyridinium are observed. Very weak peaks at 3305 and 1450 cm^{-1} indicate the presence of propylamine and/or possibly propylammonium. These observations are in good agreement with the previous crystallographic and ^{13}C NMR results,[15] which show that pyridine and propylamine are present in the sample with a ratio of 20:1, respectively. The presence of propylammonium cannot be ruled out from the NMR or diffraction data, and in fact its presence would be consistent with the reaction mechanism proposed in ref 15, where propylammonium cations are considered to be important in the nucleation of ferrierite.

Figure 5b shows an expanded region of the spectrum in which the ν_1 ring-breathing mode of pyridine is split into two components: the main component at 991 cm^{-1} and a smaller component to higher energy near 998 cm^{-1}. This splitting indicates that there are two types of pyridine in the structure. On the basis of the literature data described above for the description of pyridine vibrations, the absorption at 991 cm^{-1}

is typical of liquid or isolated molecules of pyridine, and the shoulder at 998 cm^{-1} is characteristic of hydrogen-bonded pyridine. The relative integrated areas of the two components is 90−95% and 10−5%. According to the model obtained from the crystallographic data, pyridine is located within the framework of ferrierite in both the 8-ring side channel and in the main 10-ring channel. However, these two sites cannot account for the appearance of the two Raman absorptions as the relative populations of the two sites from the crystal structure are approximately equal (1.0:0.9). Furthermore, it is predicted from the pyridine-framework distances (3.48 Å in the main channel and 3.58 Å in the side channel) that the pyridine molecules at both sites interact only weakly with the framework, and this would not typically cause a shift of the ν_1 absorbance. We believe that the shoulder at 998 cm^{-1} is associated with pyridine molecules in the main 10-ring channel being hydrogen bonded through the nitrogen to adjacent protons of propylamine or propylammonium. This conclusion is based upon the relative integrated areas of the two absorbances being in good agreement with the relative occupancies of pyridine and propylamine/propylammonium at the same site in the main channel of the structure. The crystal structure shows that the pyridine and propylamine are stacked side-on in the main channel, but the relative orientation of the nitrogen atoms in both molecules is unknown. We rule out the possibility of water−pyridine complexes being formed that could result in a similar shift of the ν_1 band because siliceous zeolites are hydrophobic, and we see no evidence from IR that the ferrierite sample contains water. Consequently, we assign the band at 991 cm^{-1} to pyridine trapped in the side and main channels of the ferrierite structure and the 998 cm^{-1} absorbance to pyridine in the main channel hydrogen bonding through its nitrogen to a proton of the propylamine or propylammonium, the precise nature of the latter organic being uncertain due to its low concentration.

With the assignment of the near-IR-FT Raman spectrum of the siliceous material, the aluminosilicate materials were then investigated. Figure 6a shows the effect on the near-IR-FT Raman spectrum of changing the Si/Al ratio from 18 to 50 to 80. Three main observations can be made.

(1) Vibrations within the 2900−2700 cm^{-1} range indicate unambiguously that propylammonium is present in the samples and that its concentration increases with the Al content. This result, combined with the elemental analyses (Table 1), which show that the sodium concentration is invariant to the Si/Al ratio, indicates that propylammonium is partially charge compensating for the framework aluminum. At the low Si/Al ratio, TGA data show that the weight loss in the temperature region above 200 °C is greater than that measured from the siliceous ferrierite, indicating that as the concentration of aluminum increases, it becomes necessary for charge neutrality to replace pyridine by more than one propylammonium cation.

(2) Vibrations near 990−1030 cm^{-1} (ring breathing) and 1595 cm^{-1} (bending mode) are characteristic of neutral pyridine. No bands are observed that could be attributed to pyridine coordinated to Lewis or Brönsted sites.

(3) The ν_1 absorbance of pyridine (Figure 6b) is split into two components, one at 991 cm^{-1} and the other at 1001 cm^{-1}, similar to those observed in siliceous ferrierite. The lower frequency band is again assigned to pyridine molecules, unperturbed by local interactions, and the higher frequency band to hydrogen-bonded pyridine molecules. The expanded ν_1 region clearly shows that the fraction of pyridine molecules interacting with proton donors is minor at low aluminum content (Si/Al = 80) and increases with aluminum content. In parallel, the intensity of the peak at 991 cm^{-1}, which is assigned to

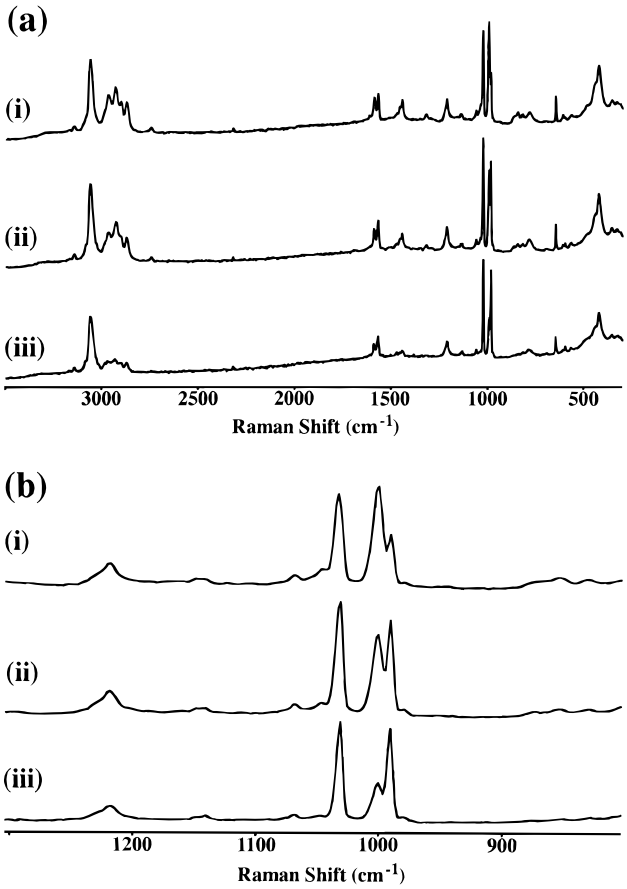

Figure 6. (a) Near-IR-FT Raman spectra taken from aluminosilicate ferrierite samples with final Si/Al molar ratios of (i) 18, (ii) 50, and (iii) 79. The corresponding expanded spectra showing the splitting of the pyridine ν_1 band are shown in (b). (*y* axis: arbitrary units.)

pyridine that does not interact with propylammonium, decreases. This is hardly surprising as the propylamine and pyridine in the main channel compete for the same site. Consequently, as the amount of framework aluminum increases and the number of propylammonium cations required to balance the charge also increases, the pyridine concentration in the main channel must decrease. The change in the relative proportions of the pyridine and propylamine as the Si/Al ratio alters is readily observed in the ^{13}C NMR spectra presented in Figure 7. Further evidence for the role of the propylammonium as a charge-compensating cation is gleaned from the Raman spectra of the as-made ferrierite (Si/Al = 18) before and after room temperature treatment under a primary vacuum. The spectra are identical, indicating that the hydrogen-bonded propylammonium−pyridine complexes are not easy to remove, consistent with the cation interacting strongly with the framework.

The similarity in the behavior of the ν_1 bands of the siliceous ferrierite and the aluminum-containing samples points to the conclusion that the splitting observed results from pyridine interacting with either propylammonium cations or propylamine neutral molecules. Indeed, the absorption at 1001 cm^{-1} cannot be attibuted to an inorganic group (Si−O containing). Indeed, inorganics are very bad scatterers as compared to organic ones and cannot be detected in our experimental conditions. We do not believe that this band results from pyridine interacting with Si−OH groups associated with internal imperfections of the zeolite because aluminosilicate zeolites are known to be less defective than their siliceous analogues, and it is generally recognized that the overall amount of silanol defects decreases with increasing Al content,[24] which is contrary to the trend observed here (intensity of the absorption at 1001 cm^{-1}

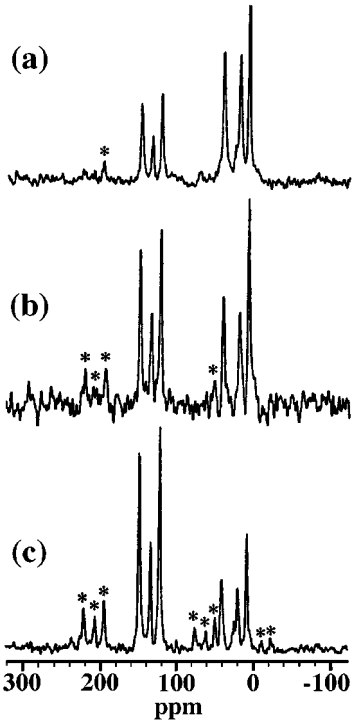

Figure 7. ^{13}C magic angle spinning NMR spectra for the samples (a) Si/Al = 80, (b) Si/Al = 50, and (c) Si/Al = 18. The peaks at 150.8, 135.7, and 123.5 ppm are assigned to pyridine, and the peaks at 41.9, 20.3, and 10.9 ppm are assigned to propylammonium. The peaks indicated by the asterisks are spinning side bands of the pyridine (*y* axis: arbitrary units).

increasing with increasing Al content). We also do not believe that bridging hydroxyls coordinating to the pyridine are responsible for the 991 cm^{-1} absorption, as in the case of H-SAPO-34,[25] as the large excess of propylamine present during the synthesis should prevent the formation of a significant number of SiOHAl groups.

The splitting of the ν_1 band occurs most probably because of the interaction of pyridine with propylammonium rather than propylamine. Indeed, we have investigated the effect on the near-IR-FT Raman spectrum of adding propylamine and propylammonium to pyridine. It was found that, even at high concentrations of propylamine, the ν_1 band of pyridine was unaffected. However, very low concentrations of propylammonium shifted the ν_1 absorbance to 1001 cm^{-1}, in good agreement with the shift observed in the ferrierite samples. In the aluminosilicate samples, the presence of propylammonium is unambiguous and its presence is necessary for charge compensation. In the siliceous ferrierite, the absorbances are so weak that it is difficult to be precise about the exact nature of the organics. Propylamine is clearly detected, and the presence of traces of propylamonium is difficult to reject. Consequently, we believe that the splitting of the ν_1 band in both the siliceous and aluminosilicate ferrierite samples results from the hydrogen bonding of the nitrogen of pyridine with a proton of propylammonium. In the siliceous sample, charge compensation for the small concentration of propylammonium cations may arise from framework defects that have been observed by photoacoustic IR measurements[26] or from fluoride anions remaining from the synthesis.

Conclusions

Zeolite synthesis commonly involves the use of organic templating molecules that become encapsulated within the pores of the inorganic framework as it crystallizes. Several papers have suggested that the FT-Raman spectroscopy, using an excitation source at 1100 nm, could be a particularly efficient tool to study these trapped molecules. The present work illustrates this possibility in the specific case of zeolitic materials of the ferrierite structure, synthesized in the presence of pyridine and propylamine.

The FT-Raman spectra of the as-synthesized siliceous ferrierite are highly resolved, enabling the characteristic vibrations of pyridine and propylamine to be independently identified. The presence of these two organic molecules within the pores of this zeolite is consistent with previous X-ray diffraction and NMR studies.[15,16] Characteristic vibrations of neutral pyridine, propylamine, and propylammonium cations are observed with the parent aluminosilicate ferrierites. The presence of cations was to be expected since positive charges were necessary to charge compensate for the Al in the framework. Strikingly, a characteristic spectroscopic fingerprint (ν_1 absorbance at 1001 cm^{-1}) indicates that the pyridine molecules are hydrogen bonded to propylamonium cations. This last observation deserves a special attention because it may aid in the understanding of why specific organic molecules are required to synthesize certain zeolitic structures. Indeed, the presence of hydrogen bonding between vicinal organic molecules may (1) decrease the average volume occupied by each templating molecule inside the porosity, (2) modify the strength of the cation/Si−O−Al interaction, and (3) alter the number of water molecules inside the porosity, thus changing the pH of the reaction in the vicinity of the organics. An understanding of all interactions between the inorganic framework and the templating molecules, as well as between the templates themselves, must be important for achieving the ultimate goal of synthesizing zeolites by design.

Acknowledgment. This work was supported by the MRL Program of the National Science Foundation under Award No. DMR-9123048. S.J.W. thanks the Ralph M. Parsons Foundation for a graduate fellowship.

References and Notes

(1) (a) Barrer, R. M. In *Hydrothermal Chemistry of Zeolites*; Academic Press: New York, 1982. (b) Davis, M. E.; Lobo, R. F. *Chem. Mater.* **1992**, *4*, 756. (c) Lok, B. M.; Cannan, T. R; Messina, C. A. *Zeolites*, **1983**, *3*, 282.

(2) Lobo, R. F.; Zones, S. I.; Davis, M. E. *J. Inclusion Phenom. Mol. Recognit. Chem.* **1995**, *21*, 47.

(3) Terasaki, O.; Oshuna, T.; Alfredsson, V.; Bovin, J. O.; Watanabe, D.; Carr, S. W.; Anderson, M. W. *Chem. Mater*. **1993**, *5*, 452.

(4) Burkett, S. L.; Davis, M. E. *J. Phys. Chem*. **1994**, *98*, 4647.

(5) Zones, S. I.; Santilli, D. S In *Proceedings of the 9th International Zeolite Conference*, Von Ballmooos, R., Higgins, J. B., Treacy, M. M., Eds.; Butterworth-Heinemann: Boston, MA, 1992; p 171.

(6) (a) Little, L. H. In *Infrared of Adsorbed Species*; Academic Press: New York, 1966. (b) Ashley, K.; Pons, S. *Chem. Rev.* **1988**, *88*, 673.

(7) (a) Egerton, T. A.; Hardin, A. H; Sheppard, N. *Can. J. Chem*. **1975**, *54*, 586. (b) Egerton, T. A.; Hardin, A. H. *Catal. Rev.-Sci. Eng*. **1975**, *11*, 71. (c) Bewick, A.; Pons, S. In *Advances in Infrared and Raman Spectroscopy*; Clark, R. J. H., Hester, R. E., Eds.; John Wiley & Sons: Chichester, 1985; Vol. 12.

(8) Bremard, C.; Bourgeard, D. *Adv. Mater.* **1995**, *7*, 10.

(9) Dutta, P. K.; Rao, K. M.; Park, J. Y. *Langmuir* **1992**, *8*, 722.

(10) Dutta, P. K.; Puri, M. *J. Phys. Chem*. **1987**, *91*, 4329.

(11) Egerton, T. A.; Hardin A. H. *Catal. Rev.-Sci. Eng*. **1975**, *11*, 71.

(12) Hendra, P.; Jones, C.; Warner, G. In *Fourier Transform Raman Spectroscopy, Instrumentation and Chemical Applications*; Ellis Horwood: New York, 1991.

(13) Burch, R.; Passingham, C.; Warnes, G. M.; Rawlence, D. J. *Spectrochim. Acta* **1990**, *2*, 243.

(14) (a) Wise, W. S.; Tschernich, R. W. *Am. Mineral.* **1976**, *61*, 60. (b) Kim, N.; Ahn, W. S.; Hong, S. B. *Microporous Mater.* **1996**, *7*, 35. (c) Kanno, N.; Miyake, M.; Sato, M. *Zeolites* **1994**, *14*, 625. (d) Li, J. Q.; Liu, G. H.; Li, J. Y. *Catal. Lett.* **1993**, *20*, 345.

(15) Weigel, S. J.; Gabriel, J.-C.; Guttierez Puebla, E.; Monge Bravo, A.; Henson, N. J.; Bull, L. M; Cheetham, A. K. *J. Am. Chem. Soc*. **1996**, *118*, 2427.

(16) Lewis, J. E., Jr.; Freyhardt, C. C.; Davis, M. E. *J. Phys. Chem*. **1996**, *100*, 5039.

(17) Kuperman, A.; Nadimi, S.; Oliver, S.; Ozin, G. A; Garces, J. M.; Olken, M. M. *Nature* **1993**, *365*, 239.

(18) Morris, R. E.; Weigel, S. J.; Henson, N. J.; Bull, L. M.; Janicke, M. T.; Chmelka, B. F.; Cheetham, A. K. *J. Am. Chem. Soc*. **1994**, *116*, 11849.

(19) Wilson, E. B., Jr. *Phys. Rev*. **1934**, *45*, 706.

(20) *The Aldrich Library of Infrared Spectra*; Pouchert, C. J., Ed.; Aldrich Chemical Co.: Milwaukee, WI, 1981.

(21) Destexhe, A.; Smets, J.; Adamowicz, L.; Maes, G. *J. Phys. Chem*. **1994**, *98*, 1506.

(22) Hendra, P. J.; Horder, J. R; Loader, E. J. *J. Chem. Soc. A* **1971**, 1766; *J. Chem. Soc. D* **1970**, 563.

(23) Hendra, P. J.; Turner, I. D. M.; Loader, E. J.; Stacey, M. *J. Phys. Chem.* **1974**, *31*, 300.

(24) Woolery, G. L.; Alemany, L. B; Dessau, R. M; Chester, A. W. *Zeolites* **1986**, *6*, 14.

(25) Smith, L.; Marchese, L.; Cheetham, A. K.; Thomas, J. M.; Wright, P. A.; Chen, J.; Morris, R. E. *Science* **1996**, *271*, 799.

(26) Davidson, A. Private communication.